

# Optimal Driving Configuration and Coil Array Geometry for Parallel Imaging

J. Wei<sup>1</sup>, P. Qu<sup>1</sup>, J. Yuan<sup>1</sup>, G. X. Shen<sup>1</sup>

<sup>1</sup>electrical & electronic engineering, the University of HongKong, HongKong, HKSAR, China, People's Republic of

**Introduction:** Parallel imaging in MRI has aroused great interests in different array designs, which from planar to volume, multi-dimension and multi-function. During practical array designs, port configuration and array geometry are very important to parallel imaging performance, especially at high field (1-2). In this research, SNR and g-factor of three coil array geometries and different port configurations were evaluated for SENSE imaging.

**Methods:** The finite difference time domain (FDTD) method was employed to solve Maxwell's curl equations for B1 sensitivity. Eight coil array models were constructed with different port configurations and geometries. The regions of interest (ROI), 47, 29, 20 cm in the left-right (l-r), posterior-anterior (p-a), and inferior-superior (i-s) directions were divided into a mesh of 218,080 Yee cells (the basic element of 3D meshes in FDTD calculations) respectively and with resolution of 5mm in each dimension. Coils were modeled by assigning the conductivity of copper ( $5.8 \times 10^7 S/m$ ) to cells in the selected regions so as to form coil array elements. The steady-state magnitudes of the magnetic flux density ( $B_1$ ) in all of the cells can be calculated. According to the principle of reciprocity (3-4), the signal intensity from each voxel is calculated as

$$SI \propto i\omega M_0 \sin\left(\gamma\tau \left| \hat{B}_1^+ \right| V\right) \left( \left( \hat{B}_1^- \right)^* \right) \quad [1]$$

where  $B_1^+$  and  $B_1^-$  are the magnitudes of the clockwise and counter-clockwise circularly polarized components of  $B_1$ , respectively. Array performance can be evaluated by the geometry factors and their SNR, which was calculated by the root-sum-of-squares (RSS) combined signals of the individual coil elements:

$$SNR_c = \sqrt{S^H \psi^{-1} S} \quad [2]$$

$$g_{\rho} = \sqrt{\left( \left( S^H \psi^{-1} S \right)^{-1} \right)_{\rho, \rho} \left( S^H \psi^{-1} S \right)_{\rho, \rho}} \quad [3]$$

with S a reformatted version of coil sensitivities, and their numbers of rows and columns equal to the number of coil elements and acceleration rate, respectively, and  $\psi$  is the noise correlation matrix.

**Results and Discussion:** In the table 1, the SNR values of three dimensional coil arrays in Fig.3 are obviously higher than one and two dimensional arrays in Fig. 1 and Fig. 2. For each kind of array, the values of SNR are all similar for different port configuration, but for g- factor, the average values of regularly accordant ports layout are a little bit lower than the other layout. The different port configuration can affect the magnetic field distribution of coil array and sensitivity, as well as the g-factor. For regularly accordant port layout as in Fig. 1a, Fig.2a and Fig.3a, the magnetic field distribution of each element in coil array is obviously separated from the others, so the sensitivity is fit for parallel imaging, the geometry noise is lower and the g-factor is improved.

**Conclusion:** The simulation results show that the regularly accordant ports position and multi-dimensional layout of coil elements will gain much higher SNR and better parallel imaging performance.

## References:

1. C.M.Collins, et al., ISMRM 11, p2391 .
2. R.F.Lee, et al., ISMRM 12, p34 .
3. C.M.Collins, M.B.Smith, Magn. Reson. Med. 45, 692 (2001).
4. J.Wang, Q.Yang, et. al. Magn. Reson. Med. 48,362 (2002).

## Acknowledgement:

This work was supported by RGC Grant, 7045/01E, and 7170/03E.

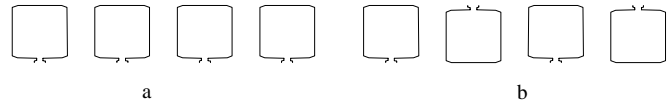


Fig. 1 one-dimensional coil array

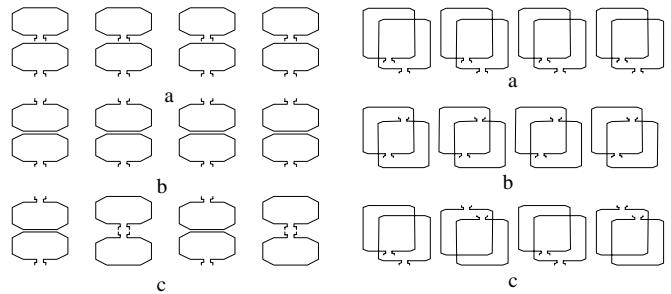


Fig. 2 two-dimensional coil array

Fig.3 three-dimensional coil array

(All Fig. a are regularly accordant port layout, Fig. b and c are relatively opposite port layout)

	Fig.1a	Fig.1b	Fig.2a	Fig.2b	Fig.2c	Fig.3a	Fig.3b	Fig.3c
Maximum SNR	13.2	13.21	24.54	24.54	24.47	67.87	68.18	68.18
Average SNR	5.13	5.16	6.69	6.70	6.696	15.55	15.54	15.55
Maximum g (R=2)	1.468	1.514	1.145	1.183	1.204	1.343	1.557	1.462
Average g (R=2)	1.032	1.032	1.011	1.012	1.012	1.029	1.043	1.033
Maximum g (R=3)	7.447	8.127	1.204	1.835	1.907	2.415	2.611	2.505
Average g (R=3)	1.130	1.145	1.038	1.039	1.040	1.088	1.094	1.092

Table 1 Comparison of SNR and g-factor of coil arrays